Detection of Discrete Interactions upon Rupture of Au Microcontacts to Self-Assembled Monolayers Terminated with −S(CO)CH_3 or −SH

Hjalti Skulason and C. Daniel Frisbie*

Contribution from the Department of Chemical Engineering and Materials Science, University of Minnesota, 421 Washington Avenue SE, Minneapolis, Minnesota 55455

Received December 30, 1999. Revised Manuscript Received July 31, 2000

Abstract: Pulloff forces were measured under solvent for Au-coated atomic force microscopy (AFM) tips in contact with −*S*-acetate-, −*O*-acetate-, −SH-, or −OH-terminated self-assembled monolayers (SAMs). The SAMs were formed by adsorption of ω-functionalized undecylphosphonic acids on metal oxide substrates. In ethanol and hexadecane, the mean force required to rupture Au/*S*-acetate microcontacts was 7 times greater than the mean force required to break Au/*O*-acetate contacts, consistent with the known affinity of S-containing functional groups for Au. Further, rupture force histograms for Au/*S*-acetate microcontacts under ethanol or hexadecane showed 0.1 nN periodicity. Rupture forces for Au/−SH microcontacts were 4 times greater than for Au/−OH microcontacts under ethanol, and the rupture force histograms showed the same 0.1 nN periodicity. We have assigned this 0.1 nN force quantum to rupture of individual chemical bonds and have estimated the bond energy to be on the order of 10 kJ/mol. The specific interaction corresponding to this energy appears to be abstraction of Au atoms from the tip surface upon pulloff. Our ability to detect these discrete interactions was a function of the solvent in which the measurements were made. For example, in water there was no difference in the mean pulloff force for Au/*S*-acetate and Au/*O*-acetate contacts and the histograms did not exhibit periodicity. In general, mean rupture forces for tip−SAM microcontacts are strongly solvent-dependent. To observe single bond rupture forces directly, we argue that the tip−substrate interfacial energy must be *negative* and larger in absolute value than the substrate−solvent and tip−solvent interfacial energies [i.e., $|\gamma_{\text{substrate-tip}}| > (\gamma_{\text{tip-solvent}} + \gamma_{\text{substrate-solvent}})$]. Otherwise, nonspecific solvent exclusion effects dominate the microcontact adhesion. These measurements show that, whereas rupture forces for tip−SAM microcontacts are solvent-dependent, these forces can be sensitive, under the right conditions, to fluctuations in the number of *discrete* chemical interactions.

Introduction

We report adhesion measurements in solvent for Au-coated atomic force microscopy (AFM) probes in contact with self-assembled monolayers (SAMs) bearing sulfur-containing terminal groups (Scheme 1). Exchanging the sulfur in the terminal group with an oxygen reduces the measured rupture force, demonstrating that the interaction of S with the Au probe is the cause of the strong adhesion. We show that rupture force distributions for hundreds of consecutive microcontacts to S-containing SAMs reveal discrete 0.1 nN force quanta, which we assign to abstraction of individual Au atoms from the surface of the Au probe. To date, there are few adhesion studies that report direct detection of rupture forces for discrete, *nonbiological* conjugations.[1] However, knowledge of the mechanical strength of individual chemical bonds can enhance understanding of the molecular dynamics of adsorption, adhesion, and self-assembly.[2]

In force microscopy studies, adhesion is quantified as a force (rather than energy/area) required to rupture the tip−sample microcontact.[3] AFM adhesion force measurements have been extensively reported[4] and recently reviewed.[5] It is now well established that rupture forces are sensitive to the chemical nature of the tip and substrate. Experiments using tips and substrates modified with SAMs have demonstrated that the measured rupture forces depend on the identity of the exposed functional groups.[3a,4c−f,h,j,k] To avoid both capillary forces associated with measurements in the ambient and the relative difficulty of working in a vacuum, AFM adhesion force

* Address correspondence to this author. E-mail: frisbie@cems.umn.edu.

(1) Hoh, J. H.; Cleveland, J. P.; Prater, C. B.; Revel, J.-P.; Hansma, P. K. *J. Am. Chem. Soc.* **1992**, *114*, 4917.

(2) Israelachvili, J. *Intermolecular and Surface Forces*; Academic Press: New York, 1992.

(3) Noy, A.; Vezenov, D. V.; Lieber, C. M. *Annu. Rev. Mater. Sci.* **1997**, *27*, 381. (b) Kendall, K. *Science* **1994**, *263*, 1720.

(4) (a) Grandbois, M.; Beyer, M.; Rief, M.; Clausen-Schaumann, H.; Gaub, H. E. *Science* **1999**, *283*, 1727. (b) Lo, Y.-S.; Huefner, N. D.; Chan, W. S.; Stevens, F.; Harris, J. M.; Beebe, T. P. *Langmuir* **1999**, *15*, 1373. (c) van der Vegte, E. W.; Hadziioannou, G. *Langmuir* **1997**, *13*, 4357. (d) Vezenov, D. V.; Noy, A.; Rozsnyai, L. F.; Lieber, C. M. *J. Am. Chem. Soc.* **1997**, *119*, 2006. (e) Sinniah, S. K.; Steel, A. B.; Miller, C. J.; Reutt-Robey, J. E. *J. Am. Chem. Soc.* **1996**, *118*, 8925. (f) Green, J.-B. D.; McDermott, M. T.; Porter, M. D. *J. Phys. Chem.* **1996**, *100*, 13342. (g) Hinterdorfer, P.; Baumgartner, W.; Gruber, H. J.; Schilcher, K.; Schindler, H. *Proc. Natl. Acad. Sci. USA* **1996**, *93*, 3477. (h) Williams, J. M.; Han, T.; Beebe, T. P. *Langmuir* **1996**, *12*, 1291. (i) Dammer, U.; Hegner, M.; Anselmetti, D.; Wagner, P.; Dreier, M.; Huber, W.; Güntherrodt, H.-J. *Biophys. J.* **1996**, *70*, 2437. (j) Noy, A.; Frisbie, C. D.; Rozsnyai, L. F.; Wrighton, M. S.; Lieber, C. M. *J. Am. Chem. Soc.* **1995**, *117*, 7943. (k) Thomas, R. C.; Houston, J. E.; Crooks, R. M.; Kim, T.; Michalske, T. A. *J. Am. Chem. Soc.* **1995**, *117*, 3830. (l) Lee, G. U.; Chrisey, L. A.; Colton, R. J. *Science* **1994**, *266*, 771. (m) Moy, V. T.; Florin, E.-L.; Gaub, H. E. *Science* **1994**, *266*, 257. (n) Florin, E.-L.; Moy, V. T.; Gaub, H. E. *Science* **1994**, *264*, 415. (o) Lee, G. U.; Kidwell, D. A.; Colton, R. J. *Langmuir* **1994**, *10*, 354. (p) Larson, I.; Drummond, C. J.; Chan, D. Y. C.; Grieser, F. *J. Am. Chem. Soc.* **1993**, *115*, 11885.

(5) Takano, H.; Kenseth, J. R.; Wong, S.-S.; O'Brien, J. C.; Porter, M. D. *Chem. Rev.* **1999**, *99*, 2845.

10.1021/ja994524e CCC: $19.00
Published on Web 09/21/2000

Scheme 1. (A) Self-assembly of alkyl phosphonic acid reagents I−IV onto metal oxides. (B) Interaction of an Au-coated AFM tip with an end-functionalized alkyl phosphonic acid SAM.

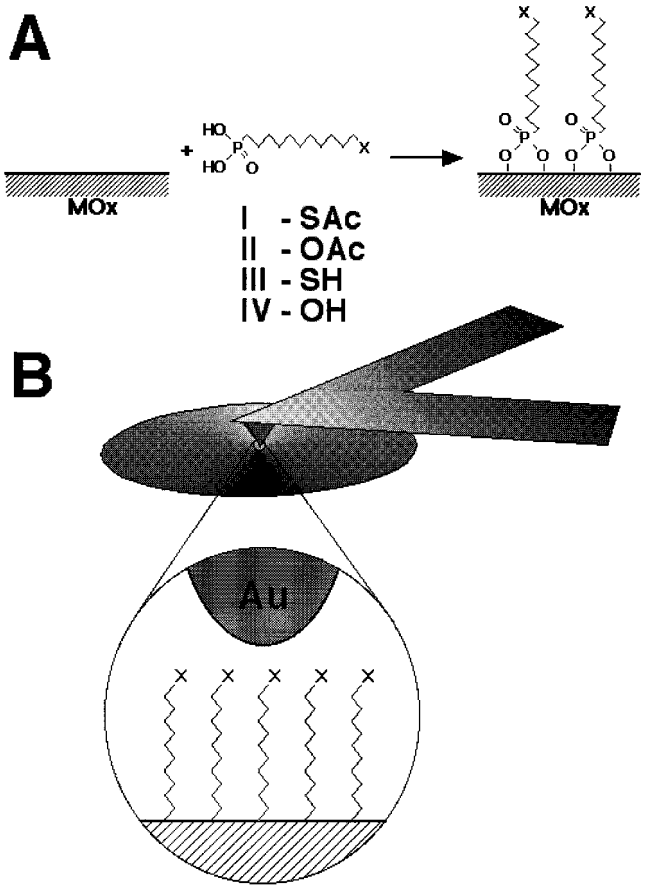

measurements are often performed in solvent. Although the measured rupture forces do depend on the nature of the exposed functional groups, the solvent often has a dramatic influence. For example, it has been reported that in ethanol 2.3 nN is required to rupture the contact between Au-coated tips and substrates functionalized with dodecylthiol.[3a] Changing the terminal group on the tip monolayer from CH_3 to COOH lowers the force to 0.3 nN, but changing the solvent from ethanol to hexadecane drops the rupture force between the CH_3-terminated surfaces to 0.07 nN. Thus the solvent can play a larger role than the tip and substrate chemistry in determining the magnitude of the adhesion force.

To the extent that a major goal of these adhesion force measurements is the determination of single bond forces, the large solvent dependence is frustrating because it masks the individual chemical interactions inside the microcontact. Indeed, there is remarkable correspondence between the measured rupture or pulloff forces (F_{pulloff}) and the predictions of continuum contact mechanics models such as Johnson−Kendall−Roberts (JKR),[6] which predict that F_{pulloff} depends on a balance of interfacial energies, namely:

$$F_{\text{pulloff}} = -\frac{3\pi}{2} R W_{\text{ad}} \tag{1}$$

$$W_{\text{ad}} = (\gamma_{\text{tip-solvent}} + \gamma_{\text{substrate-solvent}}) - \gamma_{\text{substrate-tip}} \tag{2}$$

where R is the reduced radius, W_{ad} is the work of adhesion, and $\gamma_{\text{tip-solvent}}$, $\gamma_{\text{substrate-solvent}}$, and $\gamma_{\text{substrate-tip}}$ are the tip−solvent, substrate−solvent, and substrate−tip interfacial energies. Sinniah et al.[4e] have pointed out that in many cases the tip−solvent and sample−solvent interfacial energies are relatively large, that is,

$$(\gamma_{\text{tip-solvent}} + \gamma_{\text{substrate-solvent}}) > |\gamma_{\text{substrate-tip}}| \tag{3}$$

leading to large solvent exclusion forces that are primarily responsible for microcontact adhesion. The term "solvent exclusion force" refers to a *thermodynamic (free energy) driving force*, not a mechanical force, and is associated with solvent ordering at the substrate and the tip. When $\gamma_{\text{substrate-tip}}$ is negligible compared with $(\gamma_{\text{tip-solvent}} + \gamma_{\text{substrate-solvent}})$, pulloff is determined by solvent exclusion. If the tip and substrate are chemically modified with the same molecules, it is often estimated that $\gamma_{\text{tip-solvent}} \approx \gamma_{\text{substrate-solvent}}$, so that $F_{\text{pulloff}} \propto 2\gamma_{\text{substrate-solvent}}$.[2] Although determination of $\gamma_{\text{substrate-solvent}}$ on a nanometer scale by pulloff measurements can reveal chemical heterogeneity of surfaces,[7] the often overwhelming effect of solvent exclusion is at odds with the desire (at least of chemists) to determine single bond forces.

However, experimental modifications can be made to determine single bond forces in AFM measurements. In one approach a long macromolecule is tethered to the tip and substrate and stretched until the weakest bond fails.[4a,8] This chain-stretching method has worked well for studying biological ligand−receptor interactions[4i,m−o] and should also work for studies of nonbiological bond strengths. Although the measured rupture forces in these experiments may also show solvent dependence, large solvent exclusion forces are eliminated because the tip is many nanometers away from the substrate at the point of rupture.

A second approach to detecting single bond forces is to examine tip−sample microcontacts having chemically specific interactions that are comparable with, and preferably much stronger than, the solvent exclusion contribution. That is, for the pulloff measurement to be sensitive to discrete bonds inside the microcontact, it is desirable that

$$|\gamma_{\text{substrate-tip}}| > (\gamma_{\text{tip-solvent}} + \gamma_{\text{substrate-solvent}}) \tag{4}$$

(compare with eq 3) and that $\gamma_{\text{substrate-tip}}$ be *negative*. Negative $\gamma_{\text{substrate-tip}}$ values are not sustainable for liquid−liquid interfaces, but are possible for solid−solid contacts, and reflect strong chemical bonding between the tip and substrate, increasing the pulloff force.[9] From an experimental viewpoint, $\gamma_{\text{substrate-tip}}$ must be large and negative to detect tiny rupture force variations that might occur in consecutive microcontact ruptures caused by fluctuations in the number of discrete chemical bonds formed. If $|\gamma_{\text{substrate-tip}}|$ is small, tiny rupture force variations will be difficult to detect because the contribution of the bonds to the total force is small. When $(\gamma_{\text{tip-solvent}} + \gamma_{\text{substrate-solvent}})$ is small or negligible compared with the tip−sample bonding ($\gamma_{\text{substrate-tip}}$), the rupture force directly reflects the number of chemical bonds

(6) Johnson, K. L.; Kendall, K.; Roberts, A. D. *Proc. R. Soc. London A* **1971**, *324*, 301.

(7) Frisbie, C. D.; Rozsnyai, L. F.; Noy, A.; Wrighton, M. S.; Lieber, C. M. *Science* **1994**, *265*, 2071.

(8) (a) Ortiz, C.; Hadziioannou, G. *Macromolecules* **1999**, *32*, 780. (b) Marszalek, P. E.; Oberhauser, A. F.; Pang, Y.-P.; Fernandez, J. M. *Nature* **1998**, *396*, 661. (c) Oberhauser, A. F.; Marszalek, P. E.; Erickson, H. P.; Fernandez, J. M. *Nature* **1998**, *393*, 181. (d) Rief, M.; Gautel, M.; Oesterhelt, F.; Fernandez, J. M.; Gaub, H. E. *Science* **1997**, *276*, 1109. (e) Rief, M.; Oesterhelt, F.; Heymann, B.; Gaub, H. E. *Science* **1997**, *275*, 1295.

(9) $\gamma_{\text{tip-substrate}}$ values near zero mean the adhesion is primarily caused by the solvent surface tension, whereas positive $\gamma_{\text{tip-substrate}}$ values represent unfavorable tip−sample interactions and will reduce the measured pulloff force.

formed in the microcontact, and statistical sampling may be used to estimate the rupture force associated with a single bond.[10]

In this article, we focus on this second approach for detecting single chemical bond forces. We have chosen to study the interaction of Au probes with SAMs terminated with S-containing functional groups, because Au−S interactions are strong [reported Au−thiolate bond dissociation energies are 120 kJ/mol (1.2 eV/bond),[11] roughly a third of a typical C−C bond] and facile.[12] We have prepared both *S*-acetate-[13] and thiol-terminated alkyl phosphonic acids, reagents **I** and **III**, respectively, which will adsorb to metal oxide surfaces such as In-doped Sn_2O_3 (ITO) and AlO_x via the phosphonic acid group, leaving the S-containing tail group exposed (Scheme 1). Alkyl phosphonic acids bind to metal oxides with roughly 3×10^{-10} mol/cm^2 coverages depending on the tail group.[14] The binding is believed to involve an ester linkage of the phosphonic acid with free hydroxyl groups on the substrate.[15] We have also prepared *O*-acetate- and hydroxyl-terminated alkyl phosphonic acids, reagents **II** and **IV**. Monolayers of **II** and **IV** serve as control samples in our microcontact rupture experiments, because no S is present in these films and therefore specific interactions with Au probes are not expected. Note that reagents **I** and **II** are identical except for the substitution of 1 atom, namely O for S; the same is true for reagents **III** and **IV**.

Our intention was to measure rupture forces associated with discrete Au−thiolate linkages. One article previously reported that the rupture strength of this bond is 1.4 nN.[4a] We show here that the *mean* rupture forces associated with our tip−SAM microcontacts are less than 1 nN, making it unlikely that our microcontact rupture experiments involve breaking Au−thiolate bonds. However, we do detect a 100 pN force quantum in the rupture force distributions for microcontacts to **I** and **III**. Based on energetic arguments, we have assigned this force to the abstraction of Au atoms from the surface of the AFM tip.

Before this work, the strongest specific interactions that have been probed in tip−SAM microcontacts, excluding biological interactions such as DNA duplex formation, are hydrogen bonds such as between amide-modified tips and substrates.[4c] H-bonds have energies in the range of 10−40 kJ/mol (100−400 meV/bond),[16] but no *direct* evidence for rupture of discrete H-bonds in tip−SAM microcontact pulloff experiments has been reported. As far as we are aware, our studies represent the first direct detection of discrete (nonbiological) bonds associated with tip−SAM microcontacts.

Experimental Section

Materials. 11-Bromoundecanol (98%), *p*-toluenesulfonic acid monohydrate (98.5%), hexanethiol (95%), triethyl phosphite (98%), potassium thioacetate (98%), and trimethylbromosilane (98%) were obtained from Aldrich (Milwaukee, WI) and dihydropyran (99%) was obtained from Chimica (Geel, Belgium). All solvents were of spectroscopic quality. Toluene was shaken with sulfuric acid and distilled from $CaCl_2$, and CH_2Cl_2 was distilled from P_2O_5. Absolute ethanol was obtained from Aaper Alcohol and Chemical Co. (Shelbyville, KY). Gold (99.999%) was obtained from W. E. Mowrey Co (St. Paul, MN). Aluminum (99.999%) was obtained from Alfa Esar (Ward Hill, MA). Indium−tin oxide ($R_s \leq 100\ \Omega$) coated (∼20 nm) glass slides (25 × 75 × 0.9 mm) were obtained from Delta Technologies Ltd. (Stillwater, MN). Water (18 MΩ) was filtered using a Barnstead system.

Monolayer Preparation. For IR measurements, glass slides (25 × 75 × 1 mm) were cleaned in boiling 5:1:1 $H_2O/H_2O_2/NH_4OH$, rinsed with distilled water and absolute ethanol, and dried with flowing N_2. The slides were then coated either with 5 nm of Cr followed by 100 nm of Au, or with 100 nm of Al. The native oxide formed on Al-coated slides (hereafter referred to as AlOx) was cleaned further in 100-W Ar (500 mTorr) plasma for 30 min. Slides were then immersed in a 1 mM tetrahydrofuran (THF)/AcOH (50:1) solution of the respective reagent for 12 h, followed by removal from the solution, thorough rinsing with the same solvent mixture, and drying in flowing N_2. The bilayer of **I** or **III** formed on Au-coated slides was washed with 2% tetramethylammonium hydroxide [$(CH_3)_4N^+OH^-$] in ethanol, 5% acetic acid in ethanol, and finally a copious amount of ethanol, to yield the monolayer. For force measurements, ITO[17] slides were cut into 10 × 10 mm pieces, which were cleaned in 100-W Ar plasma for 20 min followed by immersion in 1 mM THF/AcOH (50:1) solution of the respective reagent for 5 min. The substrates were then removed from the solution, rinsed thoroughly with the same solvent mixture, dried with flowing N_2, and used immediately.

Infrared Spectroscopy. Infrared spectra were recorded using a Nicolet MAGNA 550 FT-IR spectrometer equipped with Harrick Seagull reflectance apparatus and a KRS-5 polarizer. Reflection-adsorption IR spectra were acquired using p-polarized light incident angle at 84° relative to the surface normal. Typically, 2048 scans were acquired at 2 cm^{-1} resolution.

X-ray Photoelectron Spectroscopy. X-ray photoelectron spectroscopy studies were performed on a Physical Electronics PHI 5400 fitted with a 180° spherical capacitor analyzer, using a Mg X-ray source at 300 W. The S_{2p} spectra were recorded from a sampling area of ∼3 mm^2 with a takeoff angle of 55° and analyzer pass energy of 35.75 eV. Acquisition times were ∼15 min with a base pressure less than 1×10^{-9} Torr.

Force Measurements. Force measurements were performed with a Nanoscope III from Digital Instruments (Santa Barbara, CA) equipped with a fluid cell. Commercially available V-shape Si_3N_4 cantilevers with leg length of 200 μm and leg width of 20 μm were used. Both sides of each cantilever were primed with 3 nm of Cr, followed by 36 nm of Au, deposited by thermal evaporation. Au-coated cantilevers were used immediately after evaporation. Alternatively, 40 nm of Al was evaporated on both sides of a cantilever, followed by cleaning in 25-W Ar plasma for 3 min and immersion in 1 mM THF/AcOH (50:1) solution of the respective reagent for 5 min. The force constant of each lever was determined by the Cleveland method.[18] Resonance frequencies of coated cantilevers varied from 13.5 to 15.5 kHz, with the corresponding variations of the force constant between 0.048 and 0.076 N/m. Force measurements were typically performed with a Z position sweep of 100 nm at a rate 100 nm/s and ∼250 force curves collected. Force curves were analyzed using routines written in Igor Pro (Wavemetrics, Lake Oswego, OR). For each force curve, drift and nonlinearity of the photodetector was corrected by giving the contact region of the retraction curve a slope of −1. The smoothly varying

(10) The ability to achieve good rupture force statistics has been improved recently by use of tipless cantilever and a microfabricated array of tips as the substrate. Many different chemical interactions can be sampled in the same session by this method. See Green, J.-B. D.; Novoradovsky, A.; Park, D.; Lee, G. U. *Appl. Phys. Lett.* **1999**, *74*, 1489.

(11) (a) Nuzzo, R. G.; Dubois, L. H.; Allara, D. L. *J. Am. Chem. Soc.* **1990**, *112*, 558. (b) Nuzzo, R. G.; Zegarski, B. R.; Dubois, L. H. *J. Am. Chem. Soc.* **1987**, *109*, 733.

(12) (a) Ulman, A. *Chem. Rev.* **1996**, *96*, 1533. (b) Swalen, J. D.; Allara, D. L.; Andrade, J. D.; Chandross, E. A.; Garoff, S.; Israelachvili, J.; McCarthy, T. J.; Murray, R.; Pease, R. F.; Rabolt, J. F.; Wynne, K. J.; Yu, H. *Langmuir* **1987**, *3*, 932. (c) Nuzzo, R. G.; Allara, D. L. *J. Am. Chem. Soc.* **1983**, *105*, 4481.

(13) Tour, J. M.; Jones II, L.; Pearson, D. L.; Lamba, J. J. S.; Burgin, R. P.; Whitesides, G. M.; Allara, D. L.; Parikh, A. N.; Atre, S. V. J. *Am. Chem. Soc.* **1995**, *117*, 9529.

(14) (a) Gao, W.; Dickinson, L.; Grozinger, C.; Morin, F. G.; Reven, L. *Langmuir* **1996**, *12*, 6429. (b) Gardner, T. J.; Frisbie, C. D.; Wrighton, M. S. *J. Am. Chem. Soc.* **1995**, *117*, 6927. (c) Folkers, J. P.; Gorman, C. B.; Laibinis, P. E.; Buchholz, S.; Whitesides, G. M. *Langmuir* **1995**, *11*, 813.

(15) (a) Farrow, J. B.; Warren, L. J. *Colloids Surf.* **1989**, *34*, 255. (b) Ramsier, R. D.; Henriksen, P. N.; Gent. A. N. *Surf. Sci.* **1988**, *203*, 72. (c) Kuys, K. J.; Roberts, N. K. *Colloids Surf.* **1987**, *24*, 1.

(16) (a) Ben-Tal, N.; Sitkoff, D.; Topol, I. A.; Yang, A.-S.; Burt, S. K.; Honig, B. *J. Phys. Chem. B* **1997**, *101*, 450. (a) Dixon, D. A.; Dobbs, K. D.; Valentini, J. J. *J. Phys. Chem.* **1994**, *98*, 13435.

(17) Hereafter the term metal oxide (MOx) will be used for both AlOx and ITO where applicable.

(18) Cleveland, J. P.; Manne, S.; Bocek, D.; Hansma, P. K. *Rev. Sci. Instrum.* **1993**, *64*, 403.

background of the autocorrelation function was subtracted by application of a 30th order binomial filter.[19]

Synthesis. 11-*O*-Tetrahydropyranundecylbromide (Ia). To 120 mL of dry CH_2Cl_2 were added 15 g (60 mmol) 11-bromoundecanol, 6.5 mL (71 mmol) dihydropyran, and 0.3 g (1.6 mmol) *p*-toluenesulfonic acid (p-TsOH) and the solution stirred for 24 h. Then 130 mL of CH_2Cl_2 were added and the solution washed with 2 × 100 mL of saturated $NaHCO_3$ and 100 mL of saturated NaCl. Drying of the organic phase over $MgSO_4$ and solvent removal by rotary evaporation yielded dark brown oil, which was used in the next step without further purification. ^{1}H NMR (300 MHz, $CDCl_3$): δ 1.26−1.87 (m, 24 H), 3.31−3.88 (m, 6 H), 4.54 (m, 1 H).

11-Hydroxyundecyldiethylphosphonic Ester (Ib). A solution of 15.9 g (48 mmol) of **Ia** and 8.5 mL (49 mmol) of triethyl phosphite was refluxed for 12 h. After removal of ethylbromide and excess triethyl phosphite in a vacuum, the resulting oil and 0.5 g (2.6 mmol) p-TsOH were stirred in 150 mL of methanol for 1.5 h. The solution was transferred to a separatory funnel with 150 mL of diethyl ether and 100 mL of hexane and washed with 2 × 150 mL of 5% HCl and 150 mL of saturated NaCl. Drying of the organic phase over $MgSO_4$ and removal of the solvent by rotary evaporation yielded slightly yellow oil. ^{1}H NMR (300 MHz, $CDCl_3$): δ 1.25−1.85 (m, 26 H), 3.58 (t, 2 H), 4.05 (m, 4 H).

11-Bromoundecylphosphonic Acid (Ic). Ib (14 g, 45 mmol) was refluxed in 150 mL of concentrated HBr for 24 h. This mixture was then transferred to a separatory funnel along with 150 mL of $CHCl_3$ and 10 mL of methanol. The organic phase was washed with 3 × 150 mL of 5% HCl and 150 mL of saturated NaCl. Drying of the organic phase over $MgSO_4$ and removal of the solvent yielded brown oil. Repeated recrystallization from $CHCl_3$/methanol/CH_3CN gave an off-white solid. ^{1}H NMR (300 MHz, $CDCl_3$/CD_3OD): δ 1.26−1.90 (m, 20 H), 3.36 (t, 2 H).

11-*S*-Acetylundecylphosphonic Acid (I). Ic (1.1 g, 3.5 mmol) was dissolved in a solution of 30 mL of ethanol and 20 mL of THF, and to it was added 0.5 g (4.4 mmol) of potassium thioacetate. The solution was refluxed for 5 h and then transferred to a separatory funnel with 100 mL of CH_2Cl_2. The organic phase was washed with 2 × 80 mL of 5% HCl and 80 mL of saturated NaCl. The organic phase was dried over $MgSO_4$, and the solvent was removed by rotary evaporation. Crystallization from $CHCl_3$/MeOH/CH_3CN gave an off-white solid. ^{1}H NMR (300 MHz, $CDCl_3$): δ 1.25−1.82 (m 20 H), 2.31 (s, 3 H), 2.85 (t, 2 H), 8.90 (br, 2 H). IR (KBr, cm^{-1}) 2918, 2850 (C−H), 1688 (C═O), 1465, 1356 (C−H).

11-*O*-Acetylundecylphosphonic Acid (II). A solution of 1.7 g (5.4 mmol) of **Ib**, 0.9 mL (15 mmol) of AcOH, and 2.5 mL (16 mmol) of triethylamine in 50 mL dimethyl sulfoxide (DMSO) was heated to 80 °C for 12 h. Then the solution was transferred to a separatory funnel along with 120 mL of CH_2Cl_2 and 10 mL of methanol and washed with 3 × 80 mL of 5% HCl and 80 mL of saturated NaCl. Drying of the organic phase over $MgSO_4$ and removal of solvent by rotary evaporation yielded a red-brownish soft solid. Recrystallization from $CHCl_3$/methanol/CH_3CN yielded a white solid. ^{1}H NMR (300 MHz, $CDCl_3$): δ 1.20−1.78 (m, 20 H), 2.03 (s, 3 H), 4.03 (t, 2 H), 9.64 (br, 2 H). IR (KBr, cm^{-1}) 2918, 2849 (C−H), 1734 (C═O), 1645, 1369 (C−H).

11-Thioundecylphosphonic Acid (III). To a solution of 30 mL of ethanol and 20 mL of THF were added 0.7 g (2.3 mmol) of **I** and 0.56 g (10 mmol) KOH in 10 mL of water; this was stirred for 3 h under N_2. The solution was then transferred to a separatory funnel along with 100 mL of $CHCl_3$ and washed with 2 × 80 mL of 5% HCl and 80 mL of saturated NaCl. Drying of the organic phase over $MgSO_4$ and removal of the solvent by rotary evaporation yielded an off-white solid. ^{1}H NMR (300 MHz, $CDCl_3$): δ 1.25−1.82 (m, 20 H), 2.52 (m, 2 H), 10.29 (br, 2 H). IR (KBr, cm^{-1}) 1918, 2850, 1468 (C−H).

11-Hydroxyundecylphosphonic Acid (IV). A solution of 4.5 g (15 mmol) of **Ib**, 9 mL (51 mmol) of trimethylbromosilane in 50 mL of dry CH_2Cl_2 was stirred for 24 h under N_2. Then 20 mL of methanol were added and the solution stirred further for 24 h. The solution was then transferred to a separatory funnel along with 100 mL of CH_2Cl_2 and washed with 2 × 100 mL of 5% HCl and 100 mL of saturated NaCl. Drying of the organic phase over $MgSO_4$ and removal of the solvent by rotary evaporation yielded a brown, soft solid. Repeated recrystallization from $CHCl_3$/methanol/CH_3CN yielded a white solid. ^{1}H NMR (300 MHz, $CDCl_3$/CD_3OD): δ 1.21−1.67 (m, 20 H), 3.54 (t, 2 H). IR (KBr, cm^{-1}) 3190 (br, O−H), 2918, 2849, 1466 (C−H).

(19) Marchard, P.; Marmet, L. *Rev. Sci. Instrum.* **1983**, *54*, 1034.

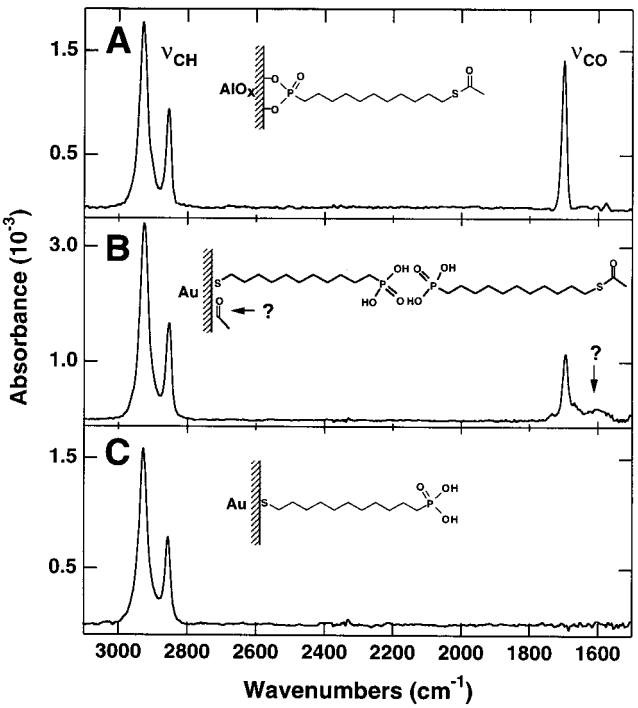

Figure 1. (A) RAIRS spectrum of **I** on AlO_x. Principal peaks correspond to C−H and C═O stretches. (B) RAIRS spectrum of an as-deposited bilayer of **I** on Au. Principal peaks correspond to C−H and C═O stretches. (C) RAIRS spectrum of a monolayer of **I** on Au, formed by washing the as-deposited bilayer with $(CH_3)_4N^+OH^-$ in ethanol. Intensity of C−H stretches is halved, whereas the C═O stretch has disappeared.

Results

Reflection−Absorption Infrared Spectroscopy. Reflection−absorption infrared spectroscopy (RAIRS) was used to characterize the structure of monolayers of **I** on AlOx and Au, and to obtain information about the binding of *S*-acetates to Au.[20] Figure 1A shows the RAIRS spectrum of a monolayer of **I** on AlOx. Symmetric and asymmetric C−H stretches are positioned at 2855 and 2928 cm^{-1}, and a carbonyl stretch is visible at 1700 cm^{-1}. Figure 1B shows the RAIRS spectrum of an as-deposited film of **I** on Au. The C−H stretches appear at 2853 and 2926 cm^{-1} as expected, but their intensity implies formation of a bilayer of **I**, presumably bound through hydrogen bonding of the phosphonic acid groups. The C═O stretching region shows an intense peak at 1695 cm^{-1} characteristic of the *S*-acetate and two weaker absorptions at 1670 and 1600 cm^{-1}. The hydrogen-bonded layer can be removed by rinsing with ethanolic $(CH_3)_4N^+OH^-$; Figure 1C shows the RAIRS spectrum of the monolayer of **I** that remains adsorbed to Au. The C−H stretching peaks have the same frequency as in the monolayer on AlOx (Figure 1A), but the C═O stretch has entirely disappeared.

X-ray Photoelectron Spectroscopy. To determine the electronic state of the sulfur atom in SAMs of **I** on MOx and Au, the S_{2p} binding energies were measured and compared with the

(20) RAIRS spectra of SAMs of **III** and **IV** were identical with those of **I** and **II** with the exception of peaks due to different end groups.

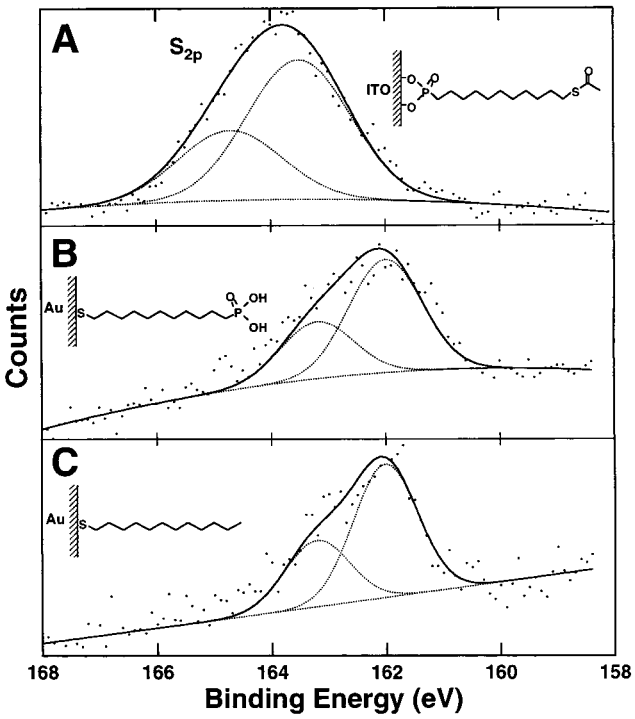

Figure 2. (A) XPS S_{2p} spectrum of **I** on ITO. Peak position corresponds to an unbound S-acetyl functional group. (B) XPS S_{2p} spectrum of a monolayer of **I** on Au. (C) XPS S_{2p} spectrum of DDT on Au. Peak is fitted with a doublet positioned at 161.9 and 163.1 eV due to $S_{2p3/2}$ and $S_{2p1/2}$ splitting with a relative area of 2:1, respectively. The peak in C is identical with the peak in B, implying that alkyl-*S*-acetates adsorb to Au to form Au−thiolates.

S_{2p} binding energies in SAMs of dodecylthiol (DDT) on Au, Figure 2. Figure 2A shows the S region of the X-ray photoelectron spectrum (XPS) for **I** on ITO. The S_{2p} peak appears as a doublet because of $S_{2p3/2}$ and $S_{2p1/2}$ splitting, positioned at 161.9 and 163.1 eV with a relative area of 2:1, respectively. These S_{2p} binding energies are typical for bulk-phase thioesters, indicating that the thioester group is intact. Figures 2B and 2C show the S_{2p} spectra for a monolayer of **I** (after rinsing with base, see Experimental) and DDT adsorbed to Au, respectively. Comparison shows that the chemical shifts are identical; the S_{2p} energies for **I** have shifted by 1.7 eV to lower binding on Au than on ITO. Adsorption of alkylthiols such as DDT give surface-bound thiolates.[11b,21] Binding of **I** to Au evidently results in cleavage of the acetyl and formation of the same surface-bound thiolate species. The S_{2p} spectrum for a bilayer of **I** on Au (not shown here) exhibited a broader peak, centered around 162.5 eV, which could be fit with a pair of doublets, representing bound thiolate and unbound *S*-acetate, in keeping with the bilayer interpretation of the RAIRS spectrum in Figure 1B.

Rupture Force Measurements. Figure 3 shows typical force curves taken with an Au-coated tip on monolayers of **I** (*S*-acetate terminated, lower trace) and **II** (*O*-acetate terminated, upper trace) on ITO under ethanol. As seen in the figure, a large difference exists in the tip−substrate rupture force measured on the two surfaces. Typical experiments involved hundreds of consecutive microcontact ruptures with the same tip. Figure 4A shows the consecutively measured rupture forces vs time for a typical Au probe contacting a monolayer of **I**; each rupture measurement was completed in 2 s. Although variance occurs in the measured force between consecutive ruptures, the mean force (0.7 nN) does not increase or decrease, implying that the tip−substrate affinity is not changing in time. Figure 4B shows that the mean rupture force also does not depend on the maximum compressive load applied to the contact.

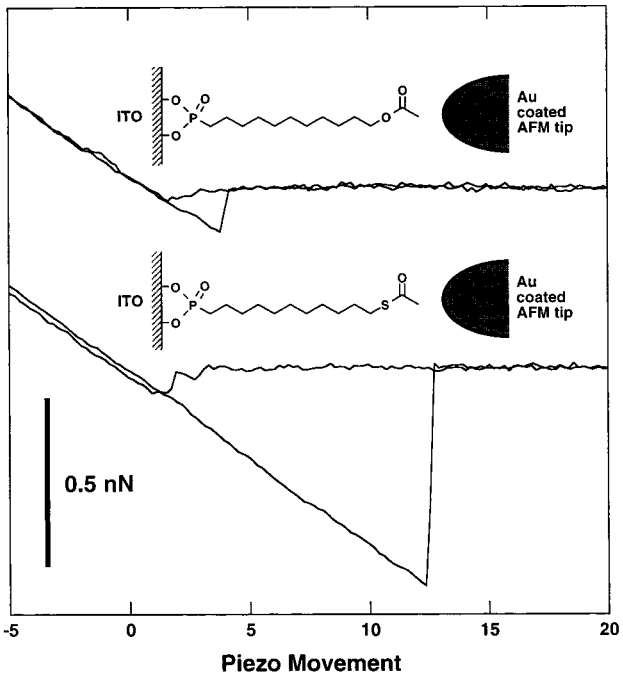

Figure 3. Representative force curves for an Au-coated AFM tip interacting with a monolayer of **I** (lower trace) and **II** (upper trace) on ITO in ethanol.

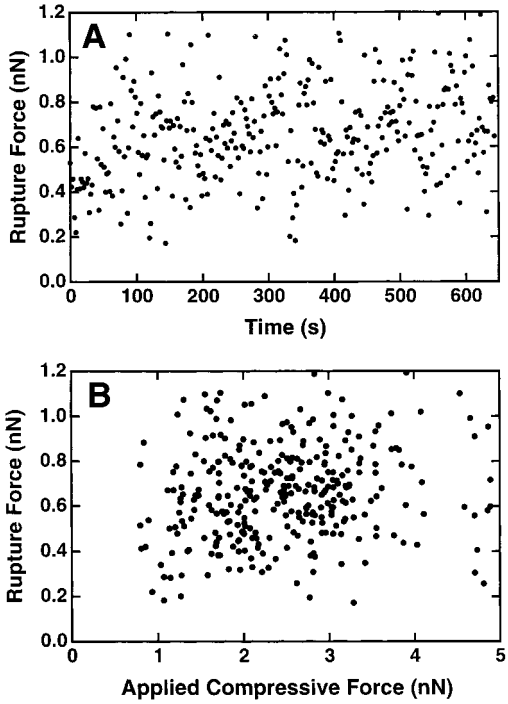

Figure 4. Rupture force between an Au-coated tip and a monolayer of **I** in ethanol as a function of time (A) and applied load (B).

Histograms (occurrence vs measured rupture force) showing the results for hundreds of consecutive microcontact ruptures between an Au probe and monolayers of **I** and **II** under ethanol are shown in Figures 5A and B. The histogram in Figure 5A corresponds to the data set in Figure 4. Inspection of Figure 5 shows that the mean rupture force ($F_{avg} \pm 1\sigma$) on the *S*-acetate-

(21) (a) Zhong, C.-J.; Brush, R. C.; Anderegg, J.; Porter, M. D. *Langmuir* **1999**, *15*, 518. (b) Gastner, D. G.; Hinds, K.; Grainger, D. W. *Langmuir* **1996**, *12*, 5083.

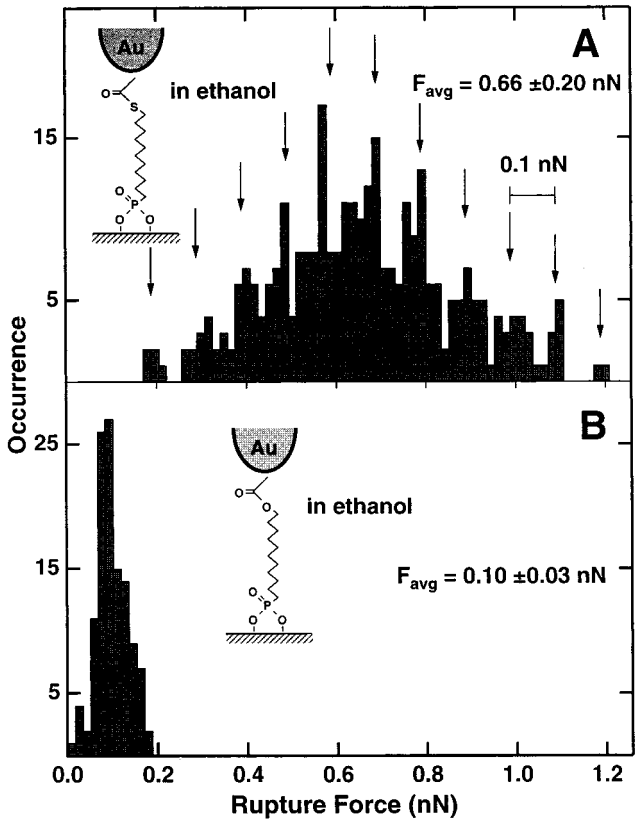

Figure 5. (A) Histogram of rupture forces between an Au-coated AFM tip and a monolayer of **I** on ITO in ethanol. Arrows point to peaks with periodicity of 0.1 nN. (B) Histogram of rupture forces between an Au-coated AFM tip and a monolayer of **II** on ITO in ethanol.

terminated film is 0.7 ± 0.2 nN (Figure 5A), but this force drops to 0.10 ± 0.03 nN on the *O*-acetate-terminated layer (Figure 5B). Thus, by exchanging the S in the *S*-acetate for O, a drop in the average force by a factor of 7 is observed. A periodicity is apparent in the *S*-acetate histogram in Figure 5A, which is highlighted by the evenly spaced arrows. This periodicity is readily apparent in the autocorrelation of the histogram (Figure 6A), which shows a sinusoidal oscillation. The period of this oscillation is 0.1 nN as indicated by the single peak in the Fourier transform of the autocorrelation (Figure 6B).

The detection of 0.1 nN quanta was characteristic for experiments performed in ethanol (and other alcohols such as methanol and propanol) and hexadecane. Figure 7 shows a histogram of rupture forces measured in hexadecane between an Au-coated tip and monolayers of **I** (Figure 7A) and **II** (Figure 7B). Again, a larger rupture force is measured for the *S*-acetate (F_{avg} = 1.2 nN)- than the *O*-acetate (F_{avg} = 0.18 nN)-terminated monolayer. Periodicity in this histogram is apparent in the sinusoidal shape of the autocorrelation function (Figure 8A), and is highlighted by the Fourier transform in Figure 8B, which shows a single peak at 0.11 nN.

Histograms from measurements performed in water are shown in Figure 9. Unlike measurements in ethanol and hexadecane, measurements in water showed no difference in the average rupture force for monolayers of **I** (F_{avg} = 2.8 ± 0.8 nN) and **II** (F_{avg} = 2.6 ± 0.7 nN). Furthermore, the average force in water was several times larger than the force measured in ethanol and hexadecane. No periodicity is observed in the histogram in Figure 9A. The autocorrelation of the histogram in Figure 9A, shown in Figure 10A, does not exhibit a constant frequency

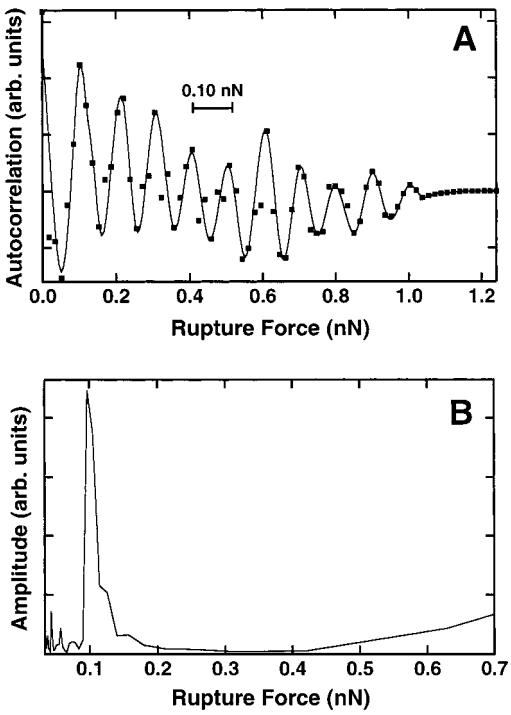

Figure 6. (A) Autocorrelation function for the histogram of rupture forces shown in Figure 5A. Oscillations have a periodicity of 0.1 nN, which is emphasized by a single peak in the Fourier Transform (B) of the autocorrelation function.

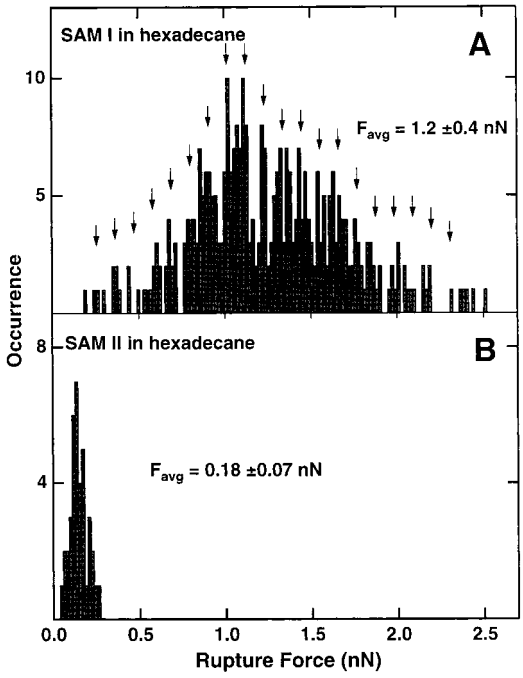

Figure 7. (A) Histogram of rupture forces between an Au-coated AFM tip and a monolayer of **I** on ITO in hexadecane. Arrows point to peaks with periodicity of 0.11 nN. (B) Histogram of rupture forces between an Au-coated AFM tip and a monolayer of **II** on ITO in hexadecane.

oscillatory behavior as emphasized by the Fourier transform of the autocorrelation in Figure 10B.

Measurements performed on a SAM of **III** showed lower average rupture force than when a SAM of **I** was used. Figure 11 shows a histogram of rupture forces between a Au-coated tip and a monolayer of **III** (Figure 11A) and **IV** (Figure 11B) in ethanol. Although rupture forces on a SAM of **III**

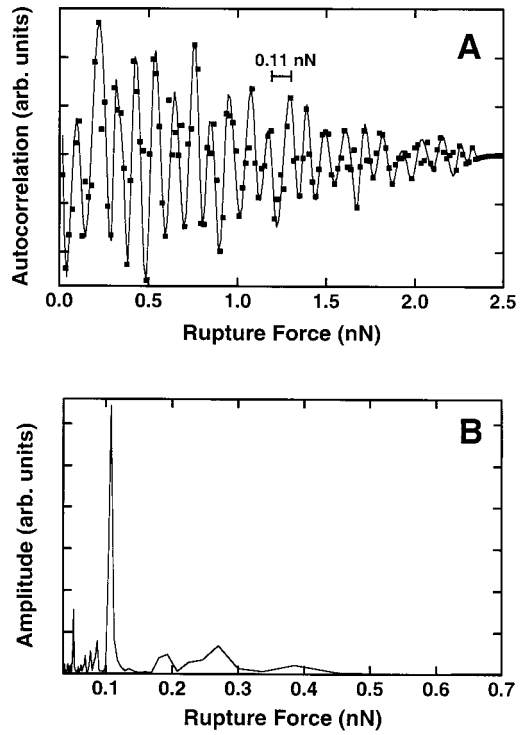

Figure 8. (A) Autocorrelation function for the histogram of rupture forces shown in Figure 7A. Oscillations have a periodicity of 0.11 nN, which is emphasized by a single peak in the Fourier Transform (B) of the autocorrelation function.

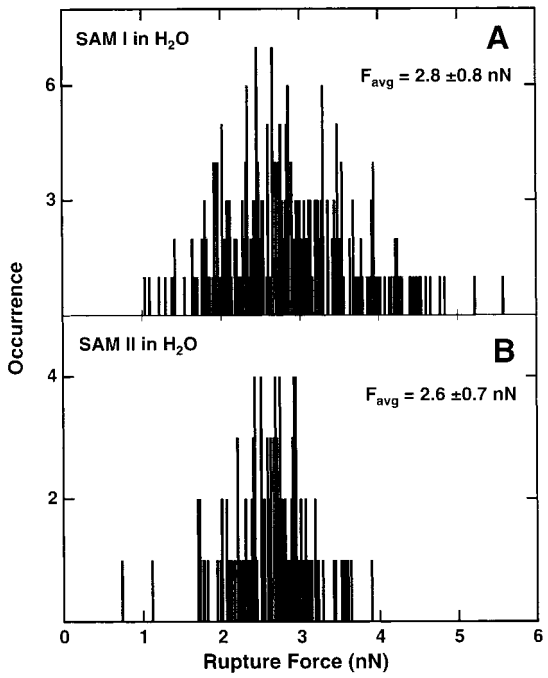

Figure 9. (A) Histogram of rupture forces between an Au-coated AFM tip and a monolayer of **I** on ITO in water. (B) Histogram of rupture forces between an Au-coated AFM tip and a monolayer of **II** on ITO in water.

(F_{avg} = 0.2 nN) are smaller than for a SAM of **I**, they are nevertheless larger than on a SAM of **IV** (F_{avg} = 0.05 nN). The histogram in Figure 11A shows the same 0.1 nN periodicity as the histograms in Figures 5A and 7A, as emphasized in the autocorrelation function (shown in Figure 12A), and the Fourier transform of the autocorrelation (Figure 12B).

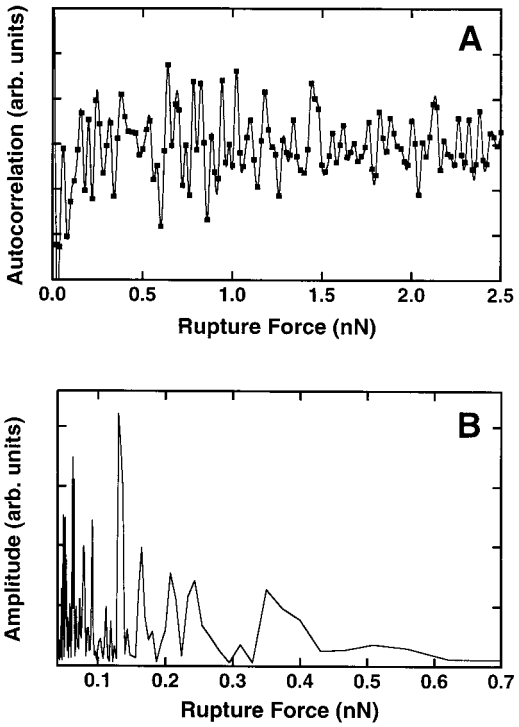

Figure 10. (A) Autocorrelation function for the histogram of rupture forces shown in Figure 9A. No periodic oscillations are observed comparable with those observed in Figures 6A and 8A, as emphasized by the complex Fourier Transform (B) of the autocorrelation function.

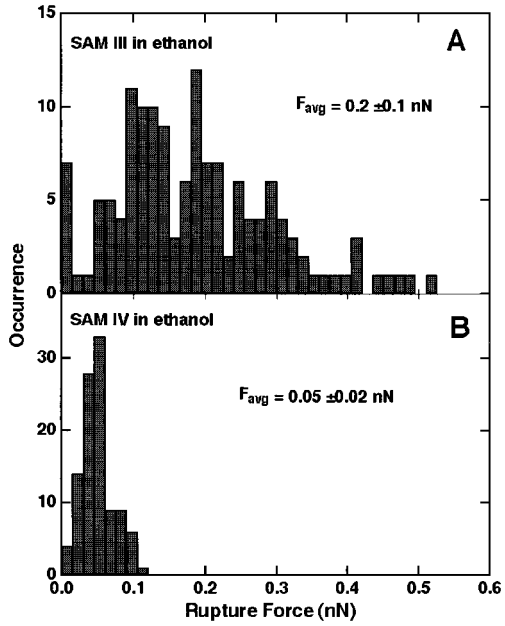

Figure 11. (A) Histogram of rupture forces between an Au-coated AFM tip and a monolayer of **III** on ITO in ethanol. (B) Histogram of rupture forces between an Au-coated AFM tip and a monolayer of **IV** on ITO in ethanol.

Discussion

Binding of I to MOx and Au. The RAIRS spectra in Figures 1A and 1C establish the presence, approximate coverage, and *orientation* of reagent **I** on metal oxide and Au surfaces. The C−H stretching absorbances in both Figures 1A and 1C are consistent with approximately monolayer coverage of **I** on MOx and Au. By comparison with typical RAIRS spectra for SAMs on Au we estimate a coverage of 3×10^{-10} mol/cm^2 (∼2 molecules/nm^2) on both MOx and Au surfaces. This coverage

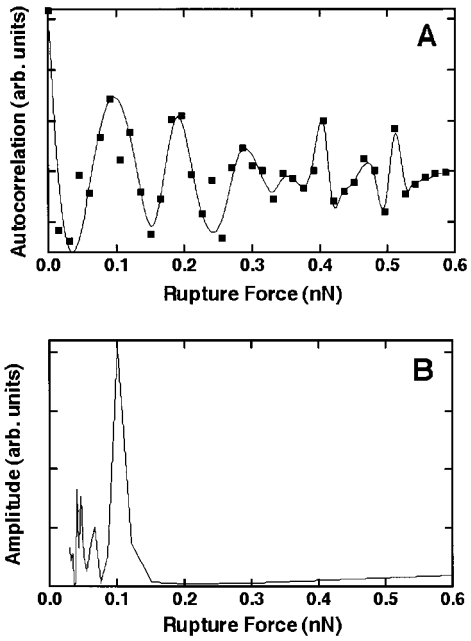

Figure 12. (A) Autocorrelation function for the histogram of rupture forces shown in Figure 11A. Oscillations have a periodicity of 0.1 nN, which is emphasized by a single peak in the Fourier Transform (B) of the autocorrelation function.

means that the alkyl chains are not close-packed, and indeed the positions of the symmetric and asymmetric C−H stretches indicate that the chemisorbed film is fluidlike, not crystalline.[22]

The most striking difference between the spectra in Figures 1A and 1C is the presence of a strong thioester carbonyl stretch in the former, and its complete absence in the latter. The large carbonyl peak in Figure 1A indicates that the thioester has not reacted and is not associated with the MOx surface, because its stretching frequency is unchanged from its position in solid IR spectra. However, the absence of the carbonyl in Figure 1C implies that the thioester group reacts with Au. We conclude that **I** binds to MOx via the phosphonic acid group and to Au via the thioester, as intended. Analogous results were obtained for reagent **III**. We have also found by RAIRS that **II** and **IV** adsorb to MOx with comparable coverages to **I**, but do not adsorb to Au, as expected.

An important question concerns the binding mechanism of **I** to Au, specifically, whether the acetyl headgroup cleaves from **I** upon adsorption, leaving a surface-bound thiolate (see sketch in Figure 1C), or remains attached to **I**, producing a surface-adsorbed acetyl moiety. Both the RAIRS and XPS results address this question. As-deposited films of **I** on Au show the presence of at least two kinds of carbonyl species in their RAIR spectra (Figure 1B), the typical thioester peak at 1695 cm^{-1} and the low intensity, broad peak at 1600 cm^{-1}, which indicates reaction of the thioester group. The C−H absorptions from the as-deposited films are roughly twice that typically found for single monolayers, indicating the formation of a bilayer. Most likely a bilayer forms by hydrogen bonding between terminal phosphonic acid groups in **I**; multilayers of alkyl phosphonates have been reported previously.[23] The CO stretch at 1695 cm^{-1} therefore corresponds to the free thioester groups that terminate the bilayer, as shown in the sketch in Figure 1B. The broad absorbance at 1600 cm^{-1} may represent a surface-adsorbed acetyl species. Upon removing the hydrogen-bonded layer by rinsing in base, the C−H absorbances drop to values consistent with a single layer and all carbonyl peaks disappear, as noted above (Figure 1C). The complete absence of any CO stretches in Figure 1C supports the model that the thermodynamically stable adsorbate is the thiolate derivative of **I**. However, metastable surface-adsorbed acetyl species may be possible, based on the data in Figure 1B.

The formation of the surface-bound thiolate derivative of **I** can be confirmed by XPS. Figures 2B and 2C show the XPS S_{2p} spectra of monolayers of **I** (after rinsing in ethanolic base) and DDT on Au. The S_{2p} chemical shifts in the two spectra are identical, meaning that the adsorbed species in both cases is a thiolate. We have also found that adsorption of alkyl *S*-acetates (no terminal phosphonic acid group) show identical spectra.

Interpretation of Microcontact Rupture Data. **Specific vs NonSpecific Interactions and the Role of Solvent**. Figures 5 and 7 clearly show that, under ethanol or hexadecane, adhesion of Au probes is significantly greater to SAMs of **I** than to SAMs of **II**. Because the only chemical difference between SAMs of **I** and **II** is the substitution of a single atom, namely O in **II** for S in **I**, the most straightforward interpretation is that the difference in adhesion arises from a specific Au−S interaction, that is, the formation of either Au−thiolate or Au−*S*-acetate bonds inside the Au-**I** microcontact. The chemical similarity of **I** and **II** makes it unlikely that there are significant differences in SAM **I** and SAM **II** solvent interfacial energies that could cause the observed differences in $F_{pulloff}$. In fact, the two monolayers showed same contact angle with water, 70°. Furthermore, control experiments using hexane thiol derivatized Au probes[24] yielded small $F_{pulloff}$ values and showed no difference in the mean $F_{pulloff}$ for SAMs of **I** and **II**. These controls demonstrate that both bare Au probes and the presence of S in the monolayer are necessary for large adhesion. They also confirm that there is no significant difference in the solvent interfacial energies of **I** and **II**. Under ethanol and hexadecane the large adhesion to SAMs of **I** must be caused by specific Au−S interactions inside the microcontact.

As expected, Figure 11 also shows that adhesion is greater to a SAM of **III** than to a SAM of **IV**. Surprisingly though, adhesion to a SAM of **III** is *lower* than to a SAM of **I**. We are not sure of the origin of this difference, because we expect that Au−thiolate bonds can form in both cases. A possible explanation is that fewer Au−thiolate bonds are formed within the Au-**III** microcontact than within the Au-**I** microcontact because of the susceptibility of the thiol group in **III** to oxidation.[25] Initially, thiols oxidize to form disulfides, but upon further oxidation sulfoxides are formed which do not bind strongly to Au. Because we observed larger mean adhesion forces for microcontacts to SAMs of **I**, we focused most of our effort on this system over SAMs of **III**.

Comparison of Figures 5, 7, and 9 shows that adhesion of Au microcontacts to SAMs of **I** and **II** is solvent-dependent. In water, the mean $F_{pulloff}$ for Au-**I** contacts (Figure 9) is greater than the mean $F_{pulloff}$ for Au-**I** contacts under either ethanol or hexadecane. Furthermore, the mean pulloff forces are the *same*

(22) Porter, M. D.; Bright, T. B.; Allara, D. L.; Chidsey, C. E. D. *J. Am. Chem. Soc.* **1987**, *109*, 3559.

(23) (a) Yang, H. C.; Aoki, K.; Hong, H.-G.; Sackett, D. D.; Arendt, M. F.; Yau, S.-L.; Bell, C. M.; Mallouk, T. E. *J. Am. Chem. Soc.* **1993**, *115*, 11855. (b) Hong, H.-G.; Mallouk, T. E. *Langmuir* **1991**, *7*, 2362. (c) Lee, H.; Kepley, L. J.; Hong, H.-G.; Akhter, S.; Mallouk, T. E. *J. Phys. Chem.* **1988**, *92*, 2597.

(24) In a control experiment, 5 mM solution of hexanethiol in ethanol was injected into the fluid cell, resulting in the average adhesion force between a SAM of **I** and an Au-coated AFM tip dropping from ∼0.6 nN to ∼0.1 nN.

(25) (a) Hutt, D. A.; Cooper, E.; Leggett, G. J. *J. Phys. Chem. B* **1998**, *102*, 174. (b) Hutt, D. A.; Leggett, G. J. *J. Phys. Chem.* **1996**, *100*, 6657. (c) Huang, J.; Hemminger, J. C. *J. Am. Chem. Soc.* **1993**, *115*, 3342.

for Au-**I** and Au-**II** contacts in water; there *appears* to be no specific Au−S interaction, contrary to the results in ethanol and hexadecane. These results point to the important role of the solvent in detecting specific chemical interactions in microcontact rupture experiments.

The ability to discriminate between *S*-acetate and *O*-acetate terminal groups in ethanol or hexadecane, but not in water, can be rationalized by consideration of substrate−solvent and tip−solvent interfacial energies and eqs 1−4. Ethanol and hexadecane completely wet monolayers of **I** and **II**, whereas water does not, suggesting that the interfacial energies of **I** and **II** with ethanol and hexadecane are smaller than with water. We have estimated these interfacial energies using pulloff force measurements because determining them from contact angle measurements was not possible. These pulloff measurements involve 'chemically symmetric contacts' in which the tip is chemically identical to the substrate, for example, a SAM of **I** on Al-coated tips in contact with a SAM of **I** on Al under ethanol. In this case, the work of adhesion can be *approximated* by $W_{ad} = 2\gamma_{substrate-solvent}$, because $\gamma_{substrate-solvent} = \gamma_{tip-solvent}$ and $\gamma_{substrate-tip} \approx 0$.[2] In ethanol we observed very little adhesion between chemically symmetric microcontacts, yielding $\gamma_{\mathbf{I}-ethanol} \approx \gamma_{\mathbf{II}-ethanol} \approx 0.1$ mJ/m^2 and $\gamma_{Au-ethanol} \approx 0.2$ mJ/m^2. Using eq 1, the mean $F_{pulloff}$ in Figure 5a, and a tip radius of ∼35 nm determined by scanning electron microscopy (SEM), we calculate $W_{ad} \approx 4.0$ mJ/m^2 for Au tips in contact with SAMs of **I** under ethanol. Consequently, from eq 2 we find $\gamma_{\mathbf{I}-Au} \approx -3.7$ mJ/m^2. The important result here is that $\gamma_{\mathbf{I}-Au}$ is *negative*, meaning there is strong adhesion between Au and the SAM of **I**, and $\gamma_{\mathbf{I}-Au}$ is a factor of 10 greater than $(\gamma_{Au-ethanol} + \gamma_{\mathbf{I}-ethanol})$. Thus, eq 4 holds and the adhesion is primarily due to Au−SAM **I** interactions and *not solvent exclusion*. We argue below that this is a necessary condition for detecting discrete bonds.

Similar results are obtained in hexadecane, although the solvent interfacial energies are larger. We estimate $\gamma_{\mathbf{I}-hexadecane} \approx \gamma_{\mathbf{II}-hexadecane} \approx 2.2$ mJ/m^2 and $\gamma_{Au-hexadecane} \approx 0.7$ mJ/m^2.[26] From Figure 7A, we determine $W_{ad} \approx 7.2$ mJ/m^2 for an Au-coated tip ($R \approx 35$ nm) in contact with a SAM of **I** under hexadecane. From eq 2, we find $\gamma_{\mathbf{I}-Au} \approx -4.3$ mJ/m^2, in good agreement with the results in ethanol. Again, $\gamma_{\mathbf{I}-Au}$ is negative and its absolute value is comparable with $(\gamma_{\mathbf{I}-hexadecane} + \gamma_{Au-hexadecane})$. Surface−solvent interfacial energies with hexadecane are higher than those with ethanol, but the $\gamma_{\mathbf{I}-Au}$ term is still the largest individual contributor to W_{ad} and consequently to $F_{pulloff}$.

By contrast, we find that $\gamma_{\mathbf{I}-Au}$ is not the dominant term in W_{ad} for Au contacts to SAMs of **I** in water. We estimate that $\gamma_{\mathbf{I}-water}$ and $\gamma_{\mathbf{II}-water}$ are ∼7 mJ/m^2 and $\gamma_{Au-water}$ is ∼5 mJ/m^2. Taking $\gamma_{\mathbf{I}-Au} \approx -4.0$ mJ/m^2 from the ethanol and hexadecane experiments, we find $(\gamma_{\mathbf{I}-water} + \gamma_{Au-water}) > |\gamma_{\mathbf{I}-Au}|$ (i.e., eq 3 holds), and adhesion is primarily due to exclusion of water from the tip−substrate contact. Although specific Au−S interactions should occur in the Au-**I** microcontact under water, the rupture force measurement is not sensitive to them because of the magnitude of the solvent exclusion effect. Consequently, there is no discrimination between mean $F_{pulloff}$ for contacts to SAMs of **I** or **II** under water (see Figure 9).

Detection of Discrete Bonds. A key result is that the histograms in Figures 5A, 7A, and 11A all show a 0.1 nN periodicity, which is highlighted by the autocorrelations and Fourier transforms in Figures 6, 8, and 12. Observation of periodicity in rupture force histograms has been reported previously and is associated with the detection of discrete unbinding events in AFM studies of biological interactions.[4i,l,n] Because we have established above that the data in Figures 5A, 7A, and 11A *must* arise from specific interactions between the tip and SAMs of **I** or **III**, we ascribe the observed periodicity to rupture of discrete bonds. Periodicity was not observed in pulloff data from SAMs of **II** or **IV** in any solvent or from SAMs of **I** in water (see Figures 9 and 10). This is expected because specific interactions of Au probes with **II** or **IV** are not anticipated, and we have argued above that measurements under water are dominated by solvent exclusion and are not sensitive to specific interactions.

The chemical identity of the bonds ruptured in Au-**I** and Au-**III** contacts cannot be determined directly, but must be inferred from the data and energetic considerations. The first important aspect of the data is that the rupture force histograms for microcontacts to the *S*-acetate-terminated SAM (**I**) show the same 0.1 nN periodicity as for contacts to the thiol-terminated SAM (**III**). This implies that the same bonds are ruptured in both cases. The second important observation is that, as shown in Figure 4A, there is no time dependence to the measured rupture force during repeated tip−substrate contacts, making it unlikely that PO_3-MO_x bonds or any bonds within **I** or **III** (e.g., C−C, C−P, P−O, C−S) are breaking. If PO_3-MO_x bonds or any bonds in **I** or **III** consistently broke, then upon repeated tip−substrate contacts the tip would become contaminated with more and more molecules or molecular fragments from the monolayer. That would lead to increasingly fewer sites available on the tip for new Au−S bonds to form, and the average rupture force would gradually decrease during the span of the experiment, which is not the case.

Thus, from the perspective of the time dependence of our measurements, the spectrum of possible weak linkages is narrowed to Au−S and Au−Au bonds. When the tip retracts, either Au−thiolate linkages break or thiolate-bound Au atoms are pulled off the tip (cohesive failure), leaving substrate-bound Au−thiolate complexes. These two possible mechanisms are shown in Scheme 2. Either mechanism would yield a 'clean' Au tip with Au atoms accessible for subsequent bond formation with S-containing functional groups in consecutive microcontacts. A potential complication with the Au abstraction mechanism in Scheme 2B is that Au atoms are left on the surface, which might block tip binding to the SAM functional groups in consecutive contacts. However, in typical experiments there is substantial drift (10 nm/s) of the tip relative to the substrate, meaning consecutive tip−SAM contacts take place on unreacted areas of the SAM.[27]

There is some evidence in the literature that cohesive failure of the Au tip coating is the correct rupture mechanism. Wasserman et al. studied the interfacial adhesion of Au films thermally evaporated onto *S*-acetate- and thiol-terminated alkylsilane monolayers.[28] Upon mechanically peeling the Au films off the monolayers, XPS analysis showed the presence of both *reduced* S atoms and *oxidized* Au atoms in a 1:1 ratio on the SAMs. Although the conditions under which the Au−S bonds are formed and ruptured in our experiments differ, this previous

(26) We acknowledge that an Au surface immediately becomes covered with organic contaminants upon exposure to air. The interfacial energies with Au that we report here reflect this adsorption to a varying degree depending on the ability of the solvent to dissolve the contaminants.

(27) Experiments with SAMs of **I** on Al-coated AFM probes in contact with Au-coated substrates in ethanol showed an average rupture force of 0.2 nN with no visible force quanta. This is consistent with the Scheme 2b mechanism, because in this case the tip rapidly becomes covered with thiolate-complexed Au, effectively blocking formation of new Au/*S*-acetate interactions in consecutive microcontacts.

(28) Wasserman, S. R.; Biebuyck, H.; Whitesides, G. M. *J. Mater. Res.* **1989**, *4*, 886.

Scheme 2. Two possible mechanisms for alkyl thiolate pulloff from an Au surface: (A) Rupture of Au−thiolate bonds or (B) rupture of thiolate-bound Au atoms from the surface

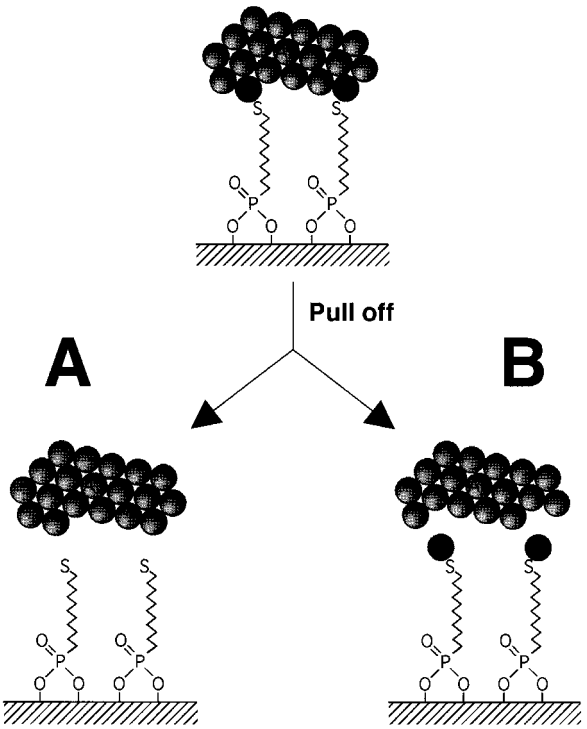

study supports a mechanism in which an Au−thiolate complex is abstracted from the Au surface (Scheme 2B).

Energetic arguments also seem to favor the Au abstraction mechanism. The bond energy associated with the force quantum we detect can be estimated by multiplying the force (0.1 nN) by an estimated rupture length (∼1 Å), giving an energy on the order of 10 kJ/mol. This is more than 10 times smaller than the reported Au−thiolate bond enthalpy (120 kJ/mol).[11] It does not seem likely that the error in the estimated rupture length could be large enough to account for such a discrepancy. In addition, in a previous report workers measured the rupture strength of an Au−thiolate bond to be 1.4 nN.[4a] This value is in good agreement with an estimated rupture force of 2 nN obtained by dividing the bond energy by 1 Å, and appears to rule out the possibility that the 0.1 nN weak link in our experiments is the Au−thiolate bond. The situation is a bit less clear if one considers that there is undoubtedly a distribution of bond enthalpies for the Au−thiolate interaction because the S atom may reside in a variety of sites with different symmetries on the Au surface; the 120 kJ/mol bond enthalpy corresponds to the minimum in the Au−S potential and a maximum Au−S bond strength. Ab initio calculations of the Au−S potential show that the Au−thiolate bond can be as small as 40 kJ/mol,[29] dropping the estimated rupture force to 0.6 nN. However, this is still large compared with our measured rupture strength of 0.1 nN.

If the Scheme 2A mechanism is excluded based on strength arguments, the question arises as to whether the Scheme 2B mechanism is consistent with a bond strength on the order of 10 kJ/mol. The cohesive energy of an Au atom on the (111) face of an Au crystal ranges from ∼180 to 540 kJ/mol depending on its surface coordination number (3−9).[30] However, it is well-known that chemisorption can weaken surface intermetallic bonding and the effect can be substantial; for example, binding of CN^- to Au in the presence of oxidizer results in appreciable etching of Au, which means the Au−Au bond energy must drop to order kT (2.4 kJ/mol at room temperature).[31] In thiolate adsorption to Au, it is well established that vacancy islands or pits form in the Au surface.[32] A few studies have suggested that this pitting is caused by partial etching of the Au; these workers found thiolate-complexed Au in the thiol deposition solution.[33] Even if the Au removed from the surface originated at step edges or other defects, this observation implies that thiolate binding can reduce the Au surface cohesion to energies near kT. Furthermore, a recent ab initio study showed that surface Au−Au bond lengths increased as much as 20% upon thiolate adsorption,[34] although Au surface cohesive energies were not reported. In a scanning tunneling microscopy (STM) study, Stranick et al. concluded that weakening of Au surface bonding facilitates surface diffusion of Au−alkylthiolate complexes at room temperature.[35] It is clear that thiolate adsorption substantially decreases surface Au bond strengths.

Moreover, weakening of surface bonding can be a function of coverage. In the adsorption of CO on Pd(100) and K on Rh-(111), for example, the adsorption enthalpy is two to three times *greater* at initial low coverage than at full coverage.[36] In thiolate adsorption on Au, the weakening of the metallic character is correlated with the charge transfer that occurs upon adsorption of the alkylthiol to the Au. For a *full-coverage* monolayer a charge of 0.4 e^- is transferred from the Au to the S.[37] However, it seems likely that density of Au−thiolate bonds in our microcontacts would correspond to less than full coverage. For a low-coverage monolayer, where dipole−dipole repulsion between adjacent Au−thiolate complexes is expected to be lower, the amount of charge transfer could be greater. That would result in further weakening of the metallic binding between the Au−thiolate complex and the surrounding Au atoms.

Based on these considerations, Au atom abstraction at energies on the order of 10 kJ/mol seems reasonable, and we favor Au atom abstraction from the tip (Scheme 2B) over Au−S bond breakage (Scheme 2A) as the mechanism for microcontact rupture. Further clarification of this issue can be brought about by detailed computer simulations of these microcontacts. In particular, important questions to be addressed include the effective rupture lengths and energies associated with removal of surface Au atoms, and how these values correlate with the

(29) Beardmore, K. M.; Kress, J. D.; Grønbech-Jensen, N.; Bishop, A. R. *Chem. Phys. Lett*. **1998**, *286*, 40.

(30) Kittel, C. *Introduction to Solid State Physics*; John Wiley & Sons: New York, 1996.

(31) (a) Zamborini, F. P.; Crooks, R. M. *Langmuir* **1997**, *13*, 122. (b) Greenwood, N. N.; Earnshaw, A. *Chemistry of the Elements*; Pergamon Press: Oxford, 1984.

(32) (a) Dishner, M. H.; Hemminger, J. C.; Feher, F. J. *Langmuir* **1997**, *13*, 2318. (b) Poirier, G. E. *Langmuir* **1997**, *13*, 2019. (c) Delamarche, E.; Michel, B.; Kang, H.; Gerber, Ch. *Langmuir* **1994**, *10*, 4103. (d) Schönenberger, C.; Sondag-Huethorst, J. A. M.; Jorritsma, J.; Fokkink, L. G. J. *Langmuir* **1994**, *10*, 611.

(33) (a) Schaaff, T. G.; Whetter, R. L. *J. Phys. Chem. B* **1999**, *103*, 9394. (b) Edinger, K.; Grunze, M.; Wöll, Ch. *Ber. Bunsen-Ges. Phys. Chem*. **1997**, *101*, 1811. (c) Sondag-Huethorst, J. A. M.; Schönenberger, C.; Fokkink, L. G. J. *J. Phys. Chem*. **1994**, *98*, 6826.

(34) Grönbeck, H.; Curioni, A.; Andreoni, W. *J. Am. Chem. Soc*. **2000**, *122*, 3839.

(35) Stranick, S. J.; Parikh, A. N.; Allara, D. L.; Weiss, P. S. *J. Phys. Chem.* **1994**, *98*, 11136.

(36) Somorjai, G. A. *Introduction to Surface Chemistry and Catalysis*; John Wiley & Sons: New York, 1994.

(37) Sellers, H.; Ulman, A.; Shnidman, Y.; Eilers, J. E. *J. Am. Chem. Soc*. **1993**, *115*, 9389.

density of step edges and point defects exposed at the Au tip surface.

As far as we are aware, the detection of periodicity or force quanta in the rupture force histograms in Figures 5A, 7A, and 11A represents the first *direct* detection of discrete, nonbiological bonds in microcontacts to SAMs. The sensitivity to discrete forces at the tip−SAM interface was achieved by keeping the solvent−tip and solvent−SAM interfacial energies low. This can be a general strategy for detecting discrete bonds at SAM interfaces, and thus it should be possible to exploit the chemical flexibility of SAMs to probe directly other discrete interactions by AFM.

Contact Area, Experimental Precision, Reproducibility. Inspection of Figures 5A and 7A shows that on average 5−6 bonds are broken in ethanol and 9−10 bonds are broken in hexadecane. It is interesting to compare these numbers with what could be expected based on the size of the contact area and the estimated surface coverage of **I**. In the JKR theory, the radius of the contact area, a, at pulloff is given by,

$$a^3 = (F_{\text{pulloff}} R)/K \tag{5}$$

where K is the elastic modulus of the tip and the substrate. However, difficulties arise in applying this formula to microcontacts because there is considerable uncertainty in K. In previous AFM studies, the contribution of the organic monolayers to K has been assumed to be negligible, and Young's modulus and the Poisson ratio for the metallic coating on the tip and substrate were used to evaluate K.[4c,j] As the measured pulloff force gets smaller, the diameter of the contact area approaches the thickness of the monolayer and this approximation for K becomes poor. Thus, eq 5 gives only a rough estimate of the contact area in the AFM measurements considered here. Using $K = 75$ GPa[38] and $R = 35$ nm (by SEM) gives $a = 0.68$ nm and an area at pulloff of 1.5 nm^2 in ethanol. With a surface coverage of 3×10^{-10} mol/cm^2, this corresponds to about 3 molecules in contact with the tip at pulloff. This number is in reasonable agreement with the data shown in Figure 5A, although, as expected, the calculation underestimates the contact area (and thus the number of bonds) because it does not take into account the deformation of the organic monolayer.

Important inferences also may be drawn from the width of the distributions in Figures 5, 7, and 9. The Q factor (Q = mean/σ) for these distributions is a measure of experimental precision and thus quantifies random variations in the microcontact rupture force caused by surface roughness, changes in tip shape, thermal energy in the lever, or inertia of the solvent. The Q factors for Au-**I** and Au-**II** contacts are nearly the same in a given solvent: in ethanol $Q_{\mathbf{I}} = 3.2$ and $Q_{\mathbf{II}} = 2.9$, in hexadecane $Q_{\mathbf{I}} = 2.9$ and $Q_{\mathbf{II}} = 2.8$, and in water $Q_{\mathbf{I}} = 3.4$ and $Q_{\mathbf{II}} = 3.7$. This implies that the parameters affecting precision are the same in Au-**I** and Au-**II** microcontact rupture experiments and that the precision is not a function of the presence or absence of specific Au−S interactions. In our view, the most likely cause of randomness in our experiments is surface roughness, which manifests in contact area variations in consecutive rupture measurements. Thus, we conclude that the contact area variations are the same for consecutive microcontacts to SAMs of **I** or **II**, and they are the same because they are predominately functions of roughness.[39]

On average, 1 of 10 Au-coated tips used in force measurements on SAMs of **I** produced rupture force histograms with measurable periodicity. The periodicity detected with these 'good' tips was 0.10 ± 0.02 nN for ethanol and hexadecane. What specific characteristics constitute a good tip are not completely clear. We speculate that atomic level structure, for example, the number of step edges, may be crucially important. The ability of a tip to distinguish between ruptures of n and $n + 1$ bonds hinges on the same bond breaking every time, which implies that the surface coordination number and site symmetry of the extracted Au atom must be consistently the same. This seems possible if, for example, a high-index face of an Au grain were exposed at the tip apex so that the step edge density was high. In addition to the tip's atomistic structure, its bulk mechanical integrity is also important to discrete bond detection. Because the measured rupture force is a sum of specific and nonspecific interactions, plastic deformation of the tip during an experiment will wash out periodicity by shifting the average adhesion due to nonspecific interactions. Thus, detection of periodicity in the force histograms requires the tip to be mechanically resilient. Certainly the high fraction (∼90%) of tips yielding histograms with similar average force but no apparent periodicity suggests that there are stringent requirements for detecting force quanta.

In conclusion, we have demonstrated detection of discrete chemical bonds in tip−SAM microcontact rupture experiments. These discrete bonds were apparent as a 0.1 nN force quantum in the force distributions for hundreds of consecutive microcontact ruptures. We have estimated that the associated bond energy is on the order of 10 kJ/mol and assigned it to the abstraction of thiolate-complexed Au atoms from the tip surface. Sensitivity of our measurements to single bond forces was achieved by making the measurements under solvents that have low interfacial energies with the SAMs. Detection of discrete interaction forces at AFM tip−SAM microcontacts is important, because the chemical versatility of these systems should allow investigation of the mechanical strength of a variety of chemical bond types. The mechanical robustness of SAM−metal contacts, in particular, may be of interest to investigators attempting to assemble metal−molecule−metal electrical junctions based on SAMs. Currently we are extending our AFM studies to the investigation of forces between charge-transfer molecules.

Acknowledgment. This work was supported by the Center for Interfacial Engineering (CIE) at the University of Minnesota.

JA994524E

(38) Where $K = (3((1 - \nu_1)/E_1 + (1 - \nu_2)/E_2)/4)^{-1}$ and ν and E are the Poisson ratio and Young's modulus, respectively, for Au and ITO. For ν and E values for Au, bulk values were used; for ITO, see Neerinck, D. G.; Vink, T. J. *Thin Solid Films* **1996**, *278*, 12.

(39) McKendry, R.; Theoclitou, M.-E.; Abell, C.; Rayment, T. *Langmuir* **1998**, *14*, 2846.